Hindawi Publishing Corporation
Advances in Meteorology
Volume 2014, Article ID 137694, 11 pages
http://dx.doi.org/10.1155/2014/137694

Research Article

The Use of Trajectory Cluster Analysis to Evaluate the Long-Range Transport of Black Carbon Aerosol in the South-Eastern Baltic Region

Steigvilė Byčenkienė, Vadimas Dudoitis, and Vidmantas Ulevicius

SRI Center for Physical Sciences and Technology, Savanorių Avenue 231, LT-02300 Vilnius, Lithuania

Correspondence should be addressed to Vidmantas Ulevicius; ulevicv@ktl.mii.lt

Received 31 March 2014; Revised 2 July 2014; Accepted 3 July 2014; Published 24 July 2014

Academic Editor: Mastura Mahmud

Trajectory cluster analysis and source-receptor models (the potential source contribution function (PSCF), concentration weighted trajectories (CWT), and trajectory source apportionment (TSA)) were applied to investigate the source-receptor relationship for the aerosol black carbon (BC) measured at the coastal site (Preila, 55.55°N, 21.04°E) during 2013. The main sources and paths of advection to the south-eastern Baltic region and its relation to black carbon concentration were identified. The 72 h backward trajectories of air masses arriving at Preila from January to December 2013 were determined and were categorized by clustering them into six clusters. Subsequently, BC levels at Preila associated with each air mass cluster during this period were analyzed. The PSCF and CWT analysis shows that, on high BC concentration days, the air masses commonly originated and passed over southern regions of Europe before arriving at Preila in winter, while a strong impact of wildfires was observed in spring.

1. Introduction

Black carbon aerosol is a byproduct of incomplete combustion of coal, biofuel, oil, gas, and residuals and isthe most efficiently light-absorbing aerosol component in the atmosphere [1, 2] strongly connected to anthropogenic sources. BC plays a major role in climate change and makes a significant contribution to anthropogenic radiative forcing [3]. BC aerosol can be transported far away from remote emission sources since its atmospheric lifetime is of the order of weeks or even days [4]. The transportation of BC on the global or regional scale potentially affects visibility in wide regions [5]. BC particles have been found to cause serious health problems as it is mostly present in the fine particle size range and therefore easily penetrates into the human respiratory tract andlater in the cardiovascular system [6, 7].

The atmospheric dynamics in the south-eastern Baltic region is conditioned by complex interactions of climatic and topographic effects. The Baltic Sea is situated in midlatitudes with strong weather variability due to westerlies with low-pressure systems passing through the region, so south-eastern Baltic region can experience both mild maritime conditions and locked up continental conditions, such as persistent high-pressure circulation, in the same area. The sources of BC aerosol vary significantly with region and time of year.

The study results [8, 9] have shown that the aerosol particle number concentration is closely related to wind speed and direction. Easterly winds from the continent might increase the aerosol BC concentrations from 20% (warm season) to 80% (cold season) versus the similar conditions with westerly winds from the seaside. Moreover, wind speed has a nonlinear relation with the concentration which decreases by about 25–35% in weak winds, including the calm conditions; however, an increased wind speed increases the concentration due to particle transportation from the continent. Temporal evolution of surface humidity has double effect on particle concentration. Dry weather pattern is favourable for strong

and turbulent surface winds lifting the aerosol particles in the atmosphere. In 90% of all high concentration events, the higher surface pressure field prevailed over the south-eastern Baltic. The large-scale flow during such episodes lied in the south western-north eastern direction over central Europe [10]. Blocking patterns or steady eddies over Europe during warm season tend to increase the meridional circulation in the middle troposphere. A significant large-scale easterly flow in the whole lower troposphere over the eastern Baltic is very favourable for accumulating aerosol particles from areas of Belarus, Russia, and Ukraine. The land/sea-breezes cycle can define local winds and influence the transport particles from/to coastal areas. The combination of low wind speeds and land/sea-breezes leads to the higher concentration of aerosol particles.

For midlatitudes long-range transport of aerosol black carbon is most abundant in winter and spring [11], when the long-range transport of emissions from wildfires from the Ukraine and European part of Russia frequently increases the particulate matter concentrations and when plumes from central and southern Europe are more liableto reach the high latitudes during winter.

Several different computational approaches have been used for solving inverse pollutant transport. Air mass back trajectory analysis is frequently used to point out the direction and sources of air pollution at a receptor site [12]. Back trajectories trace the path of a polluted air parcel backward in time and have long been used to track the history and pathway of air parcels arriving at a specific location since they were first developed in the 1940s by Petterssen (1940). Computational advances in the 1960s allowed isentropic analysis and trajectory calculations to be performed graphically on computers [13]. Trajectory clustering techniques, which assign trajectories intorepresentative spatial groups, are a popular method to combine the flow climatology and pollutant transport pathways with particle or gas measurements at a sampling station [14, 15].

The aim of this study was to investigate the transport pathways and potential sources of BC based on backward trajectories and BC concentration records in 2013. Cluster analysis was used to reveal the major pathways for different seasons as well as corresponding statistical analysis related to different clusters. Hybrid receptor models as potential source contribution function and concentration weighted trajectory were used for identification of BC source regions.

2. Data and Methods

2.1. Instrumentation. Real-time and continuous measurements of the BC mass concentration were provided by a Magee Scientific Company Aethalometer, Model AE40 Spectrum, manufactured by Optotek, Slovenia. The optical transmission of carbonaceous aerosol particles was measured sequentially at seven wavelengths λ (0.37, 0.45, 0.52, 0.59, 0.66, 0.88, and 0.95 μm). The BC mass concentration was estimated by measuring the change in transmittance of a quartz filter tape based on filtering of air. A Nafion tube diffusion dryer was attached to the inlet to mitigate the effects of humidity. The 0.88 μm wavelength is considered as the standard channel for BC measurements as at this wavelength BC is the principal absorber of light, while other aerosol components have negligible absorption at this wavelength [16]. The aethalometer output is calculated directly as the BC concentration through an internal conversion using assumed mass absorption efficiency. The aethalometer converts light attenuation to the BC mass concentration by the specific conversion factor (attenuation cross-section) (σ) of 16.6 $m^2\ g^{-1}$ of BC by the manufacturer (Aethalometer Operations manual, Magee Scientific) and may need to be adjusted when the greatest accuracy is required for a given site. It has been shown that conversion factor varies significantly, depending on the origin and the physical and chemical properties of the aerosol. The aethalometer data recorded with a 5-minute time base were compensated for loading effects using an empirical algorithm [17]. The aethalometer was equipped with an additional impactor removing the particles with the aerodynamic diameter larger than 2.5 μm. The starting time referred in this paper is Greenwich Mean Time (for local time: GMT + 2:00). The measurement precision of the aethalometer is reported to be ±100 ng BC m^{-3} with 1-minute average at a flow rate of 150 mL min^{-1} as specified in technical specifications by the manufacturer. It is sufficient for ambient total BC concentration measurement with a typical range (1–10 $\mu g\ m^{-3}$) in urban environments.

2.2. Measurement Site and Air Mass Trajectory Clustering. The Preila site (55.55N and 21.04E, 5 m above sea level) is located in the western part of Lithuania on the seashore of the Baltic Sea, on the Curonian Spit, far from urban areas (Figure 1).

There are no large sources of anthropogenic pollution of the atmosphere close to the monitoring site. One of the nearest industrial cities, Klaipeda, is at a distance of about 40 km to the north, and the other, Kaliningrad (Russia), is 90 km to the south from the site.

In order to analyze the association between trajectories and BC/OC concentration in air arriving at a Preila site air mass backward trajectory cluster analysis was used to classify trajectories into groups (clusters) of similar history, that is, similar path of advection and velocity of air flow, meaning that the errors in the individual trajectories tend to average out. The nonhierarchical clustering algorithm was used in this study.

The dataset of geographical coordinates of air parcel backward trajectories, having reached the Preila site, was calculated at 1 h intervals for a period of time between 0 to 120 h before arrival. The optimum number of trajectory clusters was obtained at an altitude of 100 m above sea level in 2013. Starting heights have been used in a number of prior publications [18, 19]. It should be noted that backward trajectories, in general, change altitude as a function of transit time and that the 100 m height is the only one at which the air arrives at the site. The selection of 100 m arriving height as the lowest level resulted from the orography around the site which is surrounded by forest and, thus, lower trajectories could be significantly influenced by the land orography.

The classification of air mass trajectories was performed using the k-means clustering technique (SPSS11.0.0) on a

FIGURE 1: Location of the Preila environmental pollution research site.

dataset consisting of 10 surface meteorological variables measured at Preila (end of the trajectory). To map the data, prior to the cluster analyses, the geographical coordinates were converted to x, y cartesian coordinates using the azimuthal equidistant projection with the central point set to geographical position of the Preila. Since this paper investigates the dependence of aerosol black carbon variation on the air mass path, the criterion for selecting the optimum trajectory clusters involved the greatest variation in BC mass concentration. So, using a cluster algorithm, the homogeneity within clusters was achieved by minimizing the angle distances [20] between the corresponding coordinates of the individual trajectories (considering the full length of each 120 h air mass backward trajectory).

The angle distance between two air mass backward trajectories was then given by

$$d_{12} = \frac{1}{n}\sum_{i=1}^{n} \cos^{-1}\left(0.5\frac{(A_1 + B_i - C_i)}{\sqrt{A_i B_i}}\right), \quad (1)$$

where

$$A_i = \left(X_1(i) - X_0\right)^2 + \left(Y_1(i) - Y_0\right)^2,$$
$$B_i = \left(X_2(i) - X_0\right)^2 + \left(Y_2(i) - Y_0\right)^2, \quad (2)$$
$$C_i = \left(X_2(i) - X_1\right)^2 + \left(Y_2(i) - Y_1\right)^2.$$

The variables X_0 and Y_0 define the position of the studied site $X_1(i)$, $Y_1(i)$ and $X_2(i)$, $Y_2(i)$ are coordinates of i segment for trajectories 1 and 2. Owing to a significant seasonal differentiation of the BC aerosol properties and the possible seasonal variation in transportation process of BC, all four seasons were analyzed.

2.3. PSCF Method. PSCF is a receptor model that incorporates meteorological information in its analysis scheme to produce a probability field that can be used to determine areas of the potential source contribution. The PSCF technique for source identification is a conditional probability that an air parcel that passed through the ijth cell had a high concentration upon arrival at the trajectory endpoint [21]. A limitation of the PSCF method is that grid cells can have the same PSCF value when sample concentration is either only slightly higher or much higher than the criterion. The criterion value of 50 percentile (median concentration) was used. As a result, it can be difficult to distinguish moderate sources from strong ones.

To calculate the PSCF, the whole geographic region covered by the backward trajectories was divided into a gridded i by j array. In this study the grid covers an area of interest defined by (40–70)N and 20W-40E with the center of Preila site (55.55°N, 21.04°E) as the midpoint and containing grid cells of 0.5° × 0.5°.

Mathematically, the PSCF is a function of location as defined by the cell indices i and j while the number of segments with endpoints that fall in the ijth cell is denoted by n_{ij}. The number of endpoints in the ijth cell associated with a trajectory that arrives at the sampling site at the same time as a corresponding measured pollutant concentration higher than an arbitrary criterion value is defined by m_{ij}. The PSCF value for the ijth cell is then

$$\mathrm{PSCF}_{ij} = \frac{m_{ij}}{n_{ij}}, \quad (3)$$

where n_{ij} is the total number of air masses falling into the ijth cell during the study period and m_{ij} is the number of segment trajectory endpoints in the ijth cell on the days where the source contribution of which was greater than the criterion value. It is important to note that a grid with no end points ($n_{ij} = 0$) cannot be identified as a source area in the analysis even though there are known emission sources in the grid cell [22].

Then the value of PSCF was interpreted as the probability where the concentration of BC higher than the creation level was related to the passage of air parcel through the ijth cell. These cells are indicative of areas of high potential contributions for BC pollutant.

2.4. Satellite Fire Products. As part of NASA's Earth Observing System, MODIS is carried on both the Terra and Aqua satellites. MODIS fire observations are madefour times a day from the Terra and Aqua platforms. The enhanced active fire algorithm uses brightness temperatures derived from the MODIS 4 and 11 μm channels. The MODIS active fire products provide information about actively burning fires and other thermal anomalies such as volcanoes and power

plants, including their location and timing, instantaneous radiative power, and smoldering ratio, presented at a spatial and temporal scales [23].

2.5. CWT Method. Since the PSCF method is known to have complications distinguishing between strong and moderate sources, the CWT model that determines the relative significance of potential sources has been additionally performed. CWT, also called a concentration field, is a function of BC concentrations that were reported every 1 h and the residence time of a trajectory arriving at Preila in each grid cell. The CWT model selected parameters were the Climate Diagnostics Center NCEP/NCAR Reanalysis archive grid data from the NWS NCEP, trajectory duration of 120 h, and the starting height of 100 and 500 m. The hourly trajectory segment endpoints for each back trajectory that corresponds to each 1 h BC were retained. For 120 h trajectory duration, there were normally 120 trajectory segment endpoints.

The geographical domain was divided into grid cells, each covering an area of $0.5^\circ \times 0.5^\circ$. The CWT is a measure of the source strength of a grid cell to the Preila site and is determined as follows [24, 25]:

$$\mathrm{CWT}_{i,j} = \frac{\sum_{T=1}^{L} C_T \tau_{i,j,T}}{\sum_{T=1}^{L} \tau_{i,j,T}}. \quad (4)$$

C_T is the 1 h BC concentration corresponding to the arrival of back trajectory T; $\tau_{i,j,T}$ is the number of trajectory segment endpoints in a grid cell (i, j) for back trajectory T divided by the total number of trajectory segment endpoints for back trajectory T; L is the total number of back trajectories over a time period (i.e., each season). Given C_T for BC, $\tau_{i,j,T}$ can be determined by counting the number of hourly trajectory segment endpoints in each grid cell for each trajectory. This was repeated for all the air mass back trajectories.

2.6. TSA Method. TSA is a statistical approach used to compute mean concentrations from various clusters to evaluate the effect of air masses from various directions on BC concentrations. In this study, the trajectory directions were defined by 6 sectors of 60° each, with sector 1 from due north and 80° east of north (see Figure 3). Equation (5) was used to calculate the mean BC concentration from sector j (C_j) and the relative contribution from sector I(%C_j). Consider

$$C_i = \frac{\sum_i^N C_i f_{ij}}{N_i},$$

$$N_i = \sum_i^N {}_1 f_{ij}, \quad (5)$$

$$\%C_i = \frac{C_i N_i}{\sum_{i=1}^{12} C_j N_j \times 100},$$

where N is the total number of trajectories, C_i is the concentration of BC in each ith trajectory, f_{ij} is the time passed through sector j for the ith trajectory, and N_i is the total time during which trajectories passed through sector [26].

3. Results

3.1. BC Concentrations. Seasonal frequency distribution of BC mass concentrations, which were evaluated from hourly average BC data at 880 nm collected by aethalometer from January to December 2013, is summarized in Figure 2. The yearly mean BC concentration in PM2.5 measured over the whole campaign at Preila was 712 ± 500 ng m^{-3}. This is comparable to previous studies of Byčenkienė et al. 2010 [27] conducted at Preila in 2008-2009 (750 ng m^{-3}).

The seasonal and diurnal variations of BC aerosols during cold and warm seasons as well as seasonal variation of BC frequency distribution are shown in Figures 2(a)–2(c). However, the pattern during cold and warm seasons is totally different; the highest concentrations were reached at different times, and higher concentrations were found during the winter period. The maximum of the diurnal variation appeared around 8:00-9:00, 15:00–17:00, and 20:00–22:00 in the warm season. The mean concentration of the hour of the day varied between 380 and 440 ng m^{-3} in warm season and between 560 and 710 ng m^{-3} in cold season. During cold season the diurnal variation shows that the BC concentrations are observed to be low during the day time while peak is observed during evening and night hours. When late night turned to early morning during warm season, there was a sharp increase in black carbon concentration, which is likely due to vehicular primary emissions during the morning rush-hour and in the afternoon (Figure 2(a)). High concentration of BC during evening hours is attributed to the boundary layer conditions. Throughout the sampling period, the lowest hourly BC value was 62 ± 30 ng m^{-3} in autumn (November). Although the seasonal mean BC in summer was lower (500 ± 360 ng m^{-3}) than in cold periods (1100 ± 780 ng m^{-3}), the highest hourly BC value was 1150 ± 540 ng m^{-3} due to anthropogenic pollution. The seasonal variation of BC (Figure 2(b)) reveals that the mean monthly concentration is maximum during January (1420 ng m^{-3}) that gradually decreases to minimum in August (440 ng m^{-3}) and then increases thereafter. As seen in Figure 2(c), main hourly BC concentrations were almost in a narrow range of 450–500 ng m^{-3} in summer. Hourly BC concentration frequency distribution usually was scattered in a wide mode range of 500–1500 ng m^{-3} in winter, 500–900 ng m^{-3} in autumn, and 450–550 ng m^{-3} in spring, corresponding to relatively high frequencies during these seasons.

3.2. Cluster Analyses of Air Mass Back Trajectories. PSCF model, CWT method, and cluster analysis were run with the seasonal data for winter (December–February), spring (March–May), summer (June–August), and autumn (September–November) in order to identify the main atmospheric circulation pathways influencing BC concentration (Figure 2). We attempted to use six clusters in all seasons providing the best representation of air mass classifications. It is seen that there are four dominant paths of air masses reaching Lithuania: from the W, NW, SW, and SE, as shown in Figure 3. The fast moving air masses were always observed from more distant W and NW regions. Members of

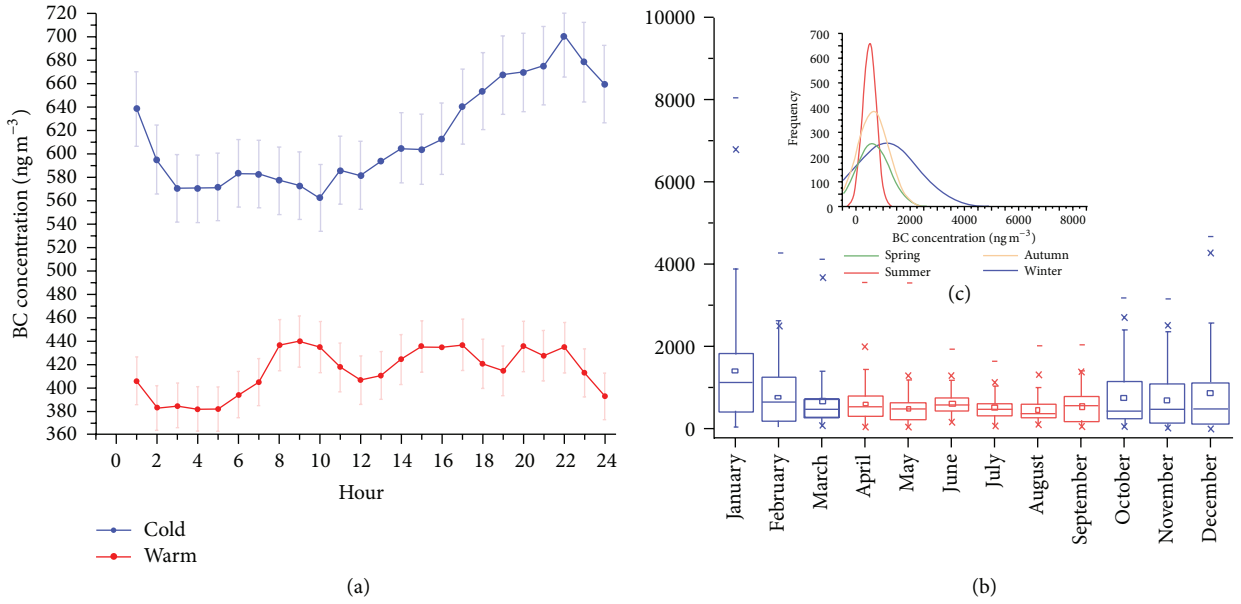

Figure 2: (a) The diurnal cycle of BC mass concentrations (on the right y-axis), (b) box plots of the mean seasonality of BC mass concentrations (lines in the middle of the boxes represent sample medians, lower and upper lines of the boxes are the 25th and 75th percentiles, and whiskers indicate the 10th and 90th percentiles, crosses indicate 5th and 95th percentiles), and (c) BC concentration frequency distribution (200 ng m^{-3} per bin) with normal distribution curve fit (line) in all clusters.

this cluster have extremely long transport patterns; some of them cross over northern Europe. Trajectories belonging to S-SW typically follow a flow pattern over Poland and Belarus. Generally such trajectories have short transport patterns, indicating slow-moving air masses. Most of the high BC level episodes within this group are probably enriched by regional and mostly local emission sources.

Figure 3 illustrates the mean trajectories (%) and BC concentration of each cluster. Trajectories from various directions had different effects on the BC concentrations. The highest BC concentration was found in cluster number 6 (winter, 3100 ± 1200 ng m^{-3}), followed by cluster number 3 (spring 1090 ± 810 ng m^{-3}) and cluster number 5 (spring, 1280 ± 1020 ng m^{-3}). Cluster number 5 may represent the effect of continental air masses from the wildfires when biomass fire events occurred during spring; thermally induced recirculation near the coastline and dust plumes from there could further contribute and influence the BC concentration level in this region (Figure 3). Except for anthropogenic emissions of fossil-fuel combustion, biomass burning including wildfires is an important contributor to the BC loading in this area.

Space-based measurements of fire radiative power are available from a number of sensors to detect when and where fire occurred and to understand thesmoke impact on the land and atmosphere. The MODIS and The Navy Aerosol Analysis and Prediction System (NAAPS) global aerosol model data were used to profile fire location maps over Lithuania, which are available as daily global fire counts. A combination of NAAPS model output and BC monitoring observations confirmed the presence of a smoke layer over Preila on 27 March (Figures 4(a)–4(c)).

During this period a mean BC increase of 15% was recorded, compared to the remaining days of March. The high BC concentrations at Preila occurred during March 27 when the 12-hour average concentrations peaked at 1100 ng m^{-3}. During March 25–30 the trajectory model indicates that wildfire emissions from Kaliningrad were "hitting" Preila. Cluster number 6 (winter) may represent the effect of air masses from southern Europe on BC concentration in winter. The lowest BC concentrations were found in cluster number 4 (autumn, 220 ± 110 ng m^{-3}) and cluster number 6 (spring, 330 ± 120 ng m^{-3}), which represent the effect of clean marine air masses from northernEurope. This air mass clusters generally originate from N and NW directions at an average altitude of around 3200 m and then sink down when traveling above the sea.

3.3. Concentration Weighted Trajectory Analysis and Potential Source Contribution Function. Figure 5 shows the distribution of weighted trajectory concentrations which gives the information on the relative contribution of source regions potentially affecting BC concentration at Preila. CWT is a function of BC concentration that was reported every 24 h and the residence time of a trajectory arriving at Preila in each grid cell. The potential source maps for BC concentration and air masses arriving at 100 m altitude at Preila during the study period for each season are given in Figure 5. Figure 5 clearly shows that air flows follow a seasonal pattern, since seasonally different CWT results were obtained. Northern Europe clusters in all seasons are associated with the lowest BC concentration values. The short clusters from SW and SE with highest BC maxima exhibit very high daily BC concentration. Short trajectories imply low wind speeds and

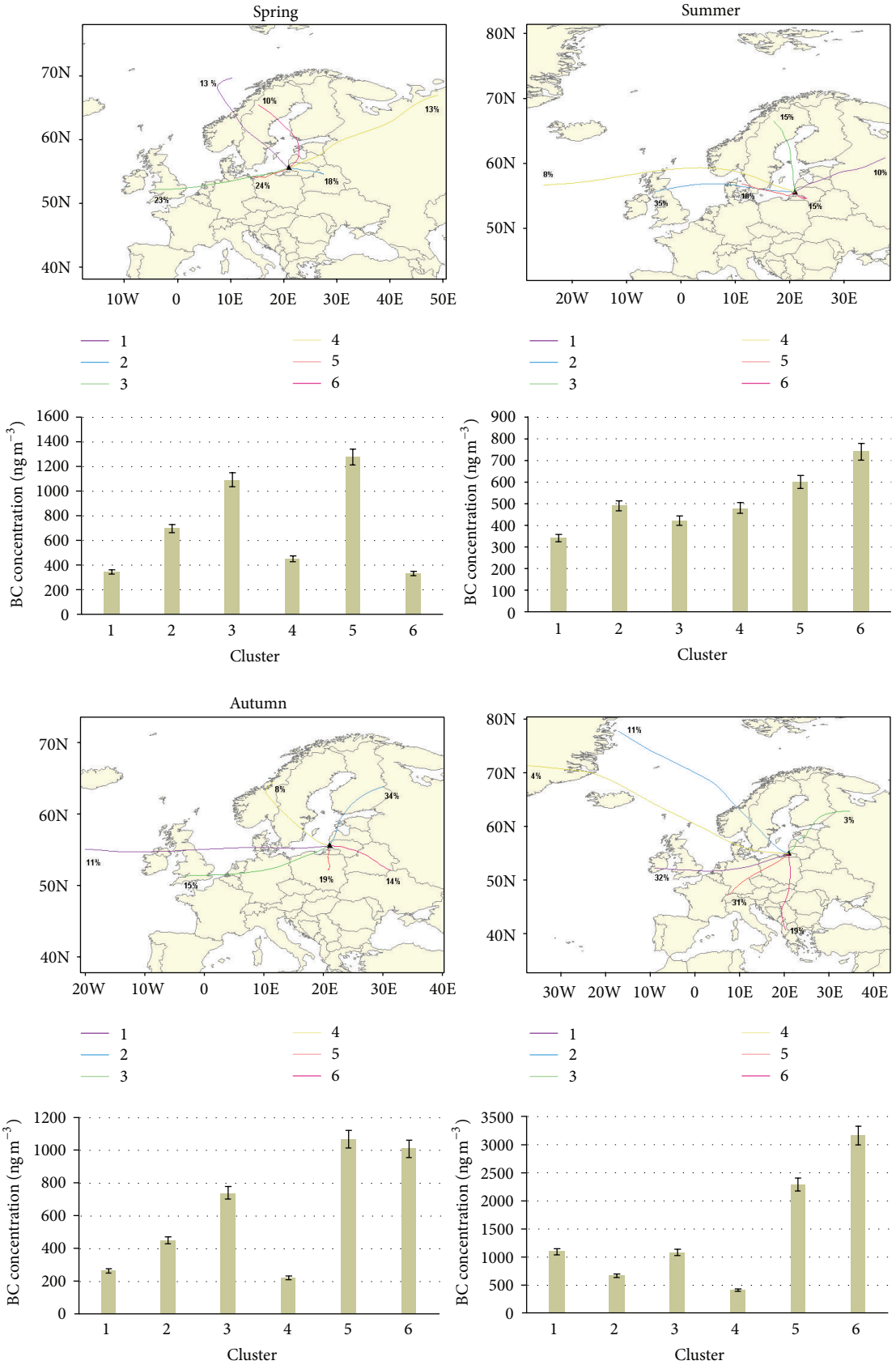

Figure 3: Trajectories representing grouping of 72 h backward trajectories of air masses over Preila into six classes for the winter, spring, summer, and autumn seasons. Mean BC concentration for all trajectory clusters arriving at Preila.

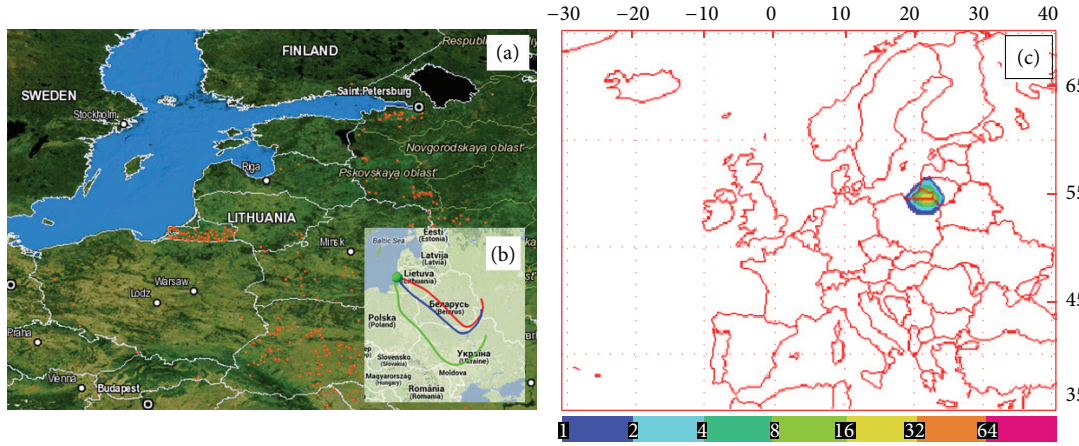

FIGURE 4: Every spring, at the end of the winter season, agricultural burning and wildfires produce large amounts of smoke in Kaliningrad (Russia), Belarus,and Ukraine. The fires usually begin in March. South westerly or easterly winds carrying the resulting smoke to Preila: (a) active fires (each red dot represents a single 1 km MODIS active fire pixel) detected during March, 2013 during high BC concentration event by the MODIS Rapid Response System, March 27 2013 (right), (b) air mass backward trajectories arriving at Preila at 50 m (red), 500 m (blue), and 1000 m (green) (left), and (c) smoke surface concentration ($\mu g\,m^{-3}$).

poor mixing ratio, so that central European countries were the greatest BC contributors to the atmosphere in Lithuania in 2013. Cells with high PSCF values (over Poland and Belarus) were the potential source regions to have effect on high BC concentration level in Preila. Figure 5 shows the map of potential PM10 (by assuming BC is component of aerosol PM10) pollution source region. Emission data bases based on officially reported data from the Member States combined in order to derive diffuse emissions to air were gridded-presented using a consistent methodology developed at EU level. Spatial analysis pointed out that maxima emissions are generated in different areas of the study domain and are more concentrated in big urban areas but homogenously distributed over Poland one of the heaviest users of district heating systems and coal as a strategic fuel in Poland in Europe. These local fossil fuel combustion activities are a major emitter of particulate matter, including BC. In 2013, heat consumption in Poland was at the level of ca. ~850 PJ, of which 560 PJ was heat demand of individual consumers, and 350 PJ was supplied from district heating systems (Figures 5 and 6 (winter)). The regions in central Europe could be a potential region for BC in Preila environment as well because highly polluted air masses are always advected to Preila. It should be noted that BC can be used as a suitable tracer to reflect the influence of long-range transported aerosol over a Preila site. The highest average contribution to the observed BC concentrations during the winter season was from the air mass cluster representing the arrival direction from Poland and Czech Republic. The most distinct air mass pattern occurs from the west, while the eastern part of Belarus and Poland (winter) is also the regions with high CWT values (>1000 $ng\,m^{-3}$). The pollution accumulated in the air masses of southern countries showsa contribution, or rather a baseline, to which local emissions (which are possibly dominant in summer and spring, Figure 6) are added. Most of the reported winter episodes in Europe were caused by long-range transport from sources of particulate matter, such as coal/wood combustion for heating [28], as well as by increased traffic emissions due to unfavorable winter driving conditions [29]. Wood burning along with domestic waste and poorest and least expensive types of fuel is probably widely existing in individual heating houses not only in Lithuania and Poland [30]. Regions over north southern Europe are always associated with the highest CWT values, but the CWT values for eastern flows are higher in summer and winter. So we have assumed that the reason for the high CWT values must be attributed to airflow loaded with BC originated from the previously mentioned countries (in winter) and biomass burning (in spring) (Figure 5).

To sum up the results, it was found that 60% of the back trajectories in the four seasons were from the west, in particular, from the northwest, while ~20% were from the north, and less than 20% were from the east. On the pathway of the air mass from the southwest there were industries, such as cement production factories, oil refining factories, and coal mines, which could emit more PM with BC. In addition, a number of fires in spring were found over Kaliningrad and the west part of Belarus and Ukraine, which might be from biomass/grass burning fires (Figure 5 (spring)). Recent findings indicate that air masses from Kaliningrad (Russia) have been shown to be optimal for higher aerosol mass concentration in northern countries and Lithuania [31]. The CWT concentration values revealed that BC concentration observed in Preila is not heavily affected by long-range transport of air masses during summer as CWT values are less variable (Figure 5). The PSCF values were calculated to evaluate the potential source contribution to BC in the atmosphere of the south-eastern Baltic sea region, based on all 72 h back trajectories arriving at the sampling site at 12:00 (local time) every day during the campaign (Figure 6).

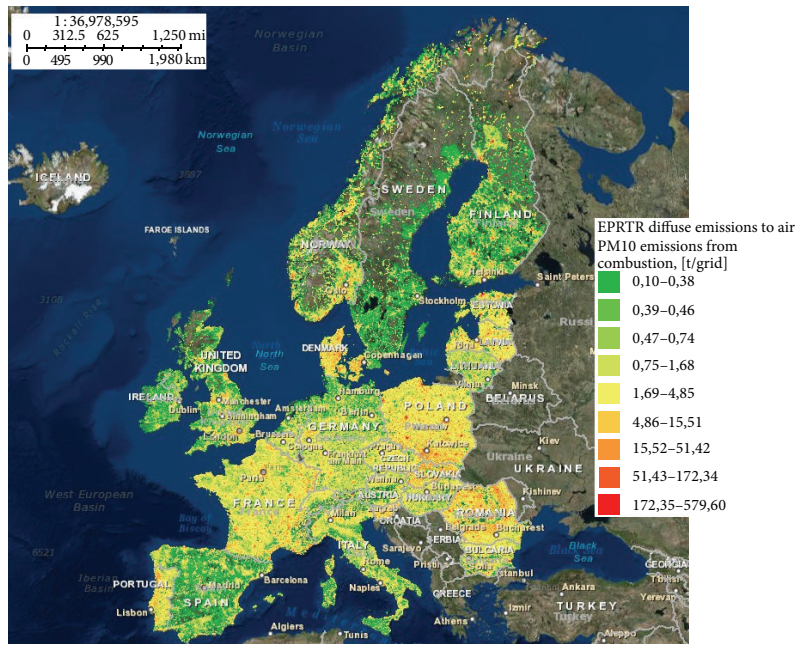

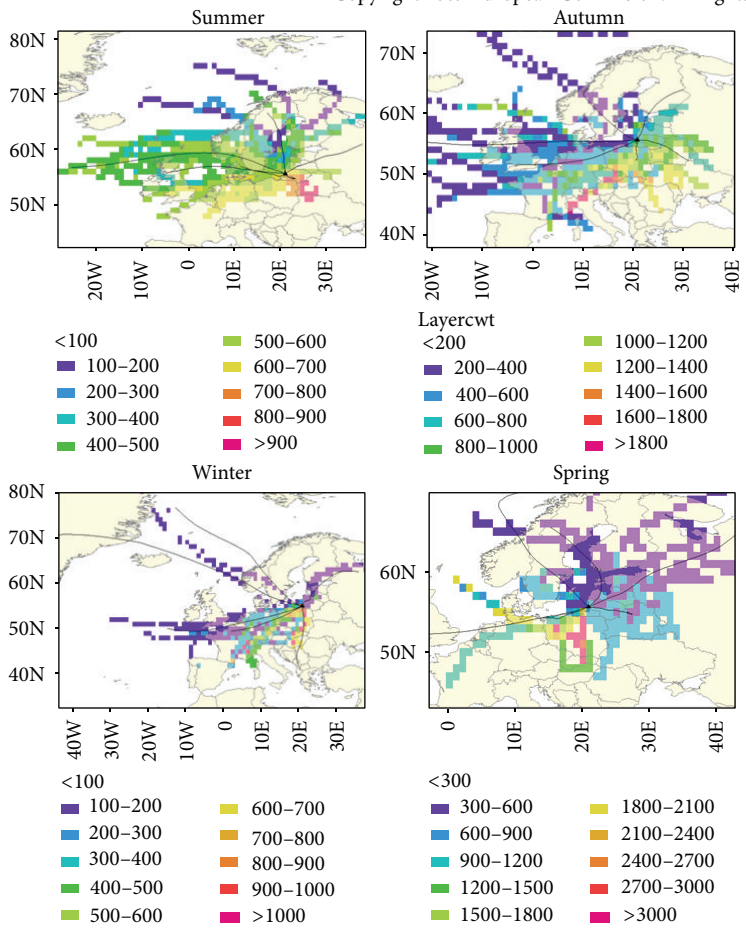

Figure 5: PM10 emissions from diffuse releases in a spatial resolution of $5 \times 5\,\text{km}^2$, t/grid; seasonal variations of the CWT maps for BC arriving at 100 m altitude at Preila in winter, spring, summer, and autumn.

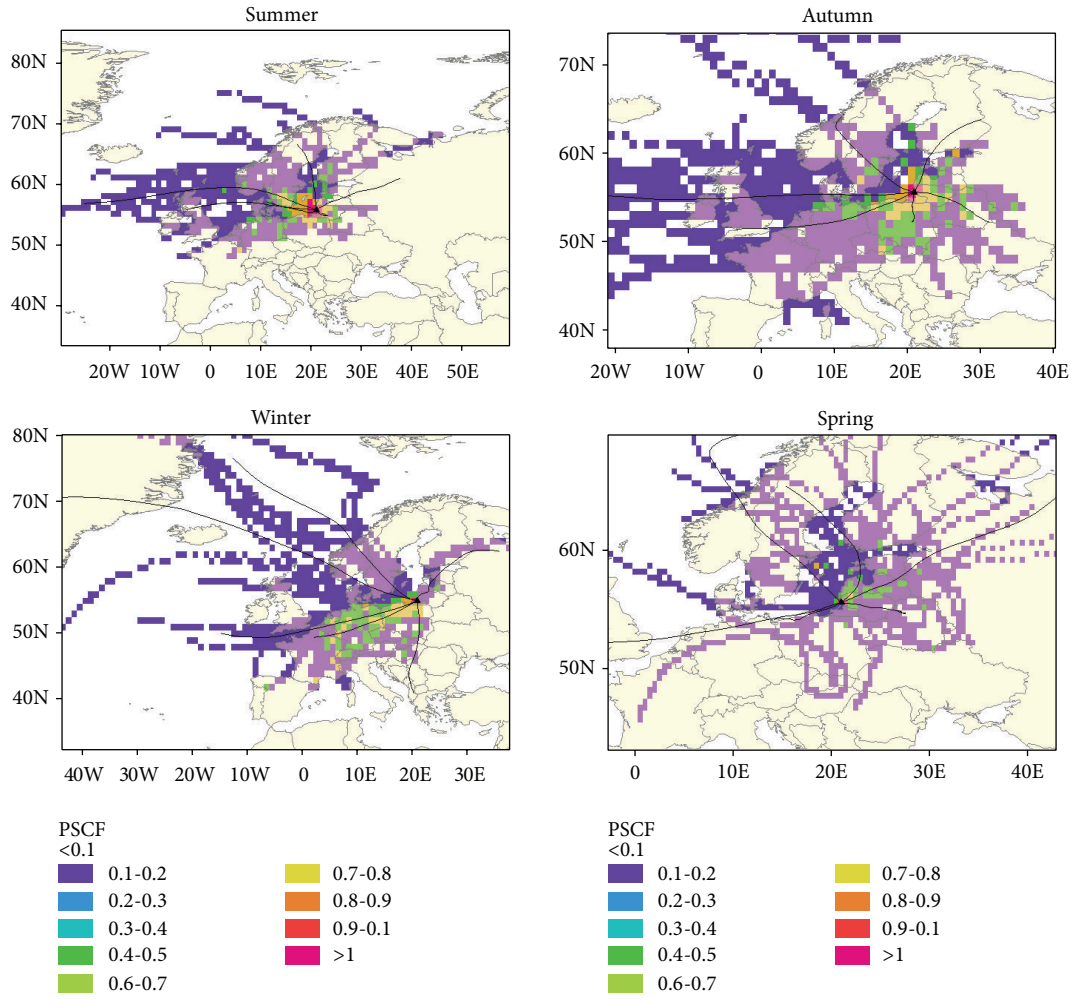

Figure 6: Seasonal variations of the potential source maps for BC arriving at 100 m altitude at Preila in winter, spring, summer, and autumn.

According to the results in the PSCF analysis, four potential source areas were identified as having important contributions to BC at Preila: northerly, northwesterly, southerly, and westerly pathways. During winter, flows from the western were responsible for picking up air pollution over the continent of Europe and then transporting them northward a long distance. On the contrary, the potential source contribution factors (0.9-1) showed local areas pollution in summer and spring.

4. Conclusions

In this study, air mass backward trajectory cluster analysis, CWT and PSCF methods were used to investigate the transport pathways and potential sources of BC in the south-eastern Baltic region. PSCF analysis in conjunction with satellite information identified little extra chunkof Russia stuck between Lithuania and Poland onthe Baltic Sea (Kaliningrad) as the main source areaaffecting the Preila site during wildfires in spring. These events significantly elevated the annual BC levels observed in the south-eastern Baltic region. An annual increase in BC concentration in spring suggests that controlling biomass burning could be an efficient way to decrease aerosol particle pollution in the south-eastern Baltic region. Six clusters were generated from backward trajectory cluster analysisfor different seasons. These clusters provided a main mechanism of transporting BC to Preila. The high BC aerosol mass concentration at Preila is a reflection of the high emission of fossil-fuel combustion in Lithuania and southern part of close countries (Poland) when air flows transported high-concentration of BC to the coastal site.

Conflict of Interests

The authors declare that they have no competing interests as defined by Advances in Meteorology or other interests that might be perceived to influence the results and discussion reported in this paper.

Acknowledgment

This work was supported by the Lithuanian-Swiss Cooperation Programme “Research and Development” project AEROLIT (no. CH-3-ŠMM-01/08).

References

[1] N. Ramanathan, M. Lukac, T. Ahmed et al., "A cellphone based system for large-scale monitoring of black carbon," *Atmospheric Environment*, vol. 45, no. 26, pp. 4481–4487, 2011.

[2] X.-F. Huang, T.-L. Sun, L.-W. Zeng, G.-H. Yu, and S.-J. Luan, "Black carbon aerosol characterization in a coastal city in South China using a single particle soot photometer," *Atmospheric Environment*, vol. 51, pp. 21–28, 2012.

[3] Intergovernmental Panel on Climate Change (IPCC), "Climate change 2013: the physical science basis," IPCC 5th Assessment Report, 2013.

[4] Intergovernmental Panel on Climate Change (IPCC), *Climate Change 2007: The Physical Science Basis*, 2007.

[5] R. Damoah, N. Spichtinger, C. Forster et al., "Around the world in 17 days—Hemispheric-scale transport of forest fire smoke from Russia in May 2003," *Atmospheric Chemistry and Physics*, vol. 4, no. 5, pp. 1311–1321, 2004.

[6] P. J. Anderson, J. D. Wilson, and F. C. Hiller, "Respiratory tract deposition of ultrafine particles in subjects with obstructive or restrictive lung disease," *Chest*, vol. 97, no. 5, pp. 1115–1120, 1990.

[7] C. P. Yu and G. B. Xu, *Deposition of Hygroscopic Aerosol Particles in Growing Human Lungs. Deposition and Clearance of Aerosols in the Human Respiratory Tract*, 1987.

[8] K. Plauškaitė, A. Gaman, K. E. J. Lehtinen, G. Mordas, V. Ulevičius, and M. Kulmala, "A comparison study of meteorological parameters, trace gases and nucleation events in Preila and Hyytiala," *Environmental and Chemical Physics*, vol. 25, no. 2, pp. 60–69, 2003.

[9] V. Ulevicius, S. Byčenkienė, V. Remeikis et al., "Characterization of aerosol particle episodes in Lithuania caused by long-range and regional transport," *Atmospheric Research*, vol. 98, no. 2–4, pp. 190–200, 2010.

[10] E. Rimkus, G. Stankevičius, and A. Bukantis, "Effects of meteorological factors on PM2.5 concentrations at Preila monitoring station," *Geografija*, vol. 42, pp. 56–64, 2006.

[11] S. Saarikoski, M. Sillanpää, M. Sofiev et al., "Chemical composition of aerosols during a major biomass burning episode over Northern Europe in spring 2006: experimental and modelling assessments," *Atmospheric Environment*, vol. 41, no. 17, pp. 3577–3589, 2007.

[12] R. S. San José, A. Stohl, K. B. Karatzas, T. Bohler, P. James, and J. L. Pérez, "A modelling study of an extraordinary night time ozone episode over Madrid domain," *Environmental Modelling and Software*, vol. 20, no. 5, pp. 587–593, 2005.

[13] E. F. Danielsen and R. Bleck, "Research in four-dimensional diagnosis of cyclonic storm cloud system," AFCRL Report vol. 67-0617, AFCRL, Bedford, Mass, USA, 1967.

[14] S. R. Dorling, T. D. Davies, and C. E. Pierce, "Cluster analysis: a technique for estimating the synoptic meteorological controls on air and precipitation chemistry—method and applications," *Atmospheric Environment A: General Topics*, vol. 26, no. 14, pp. 2575–2581, 1992.

[15] A. Sirois and J. W. Bottenheim, "Use of backward trajectories to interpret the 5-year record of PAN and O_3 ambient air concentrations at Kejimkujik National Park, Nova Scotia," *Journal of Geophysical Research*, vol. 100, no. 2, pp. 2867–2881, 1995.

[16] B. A. Bodhaine, "Aerosol absorption measurements at Barrow, Mauna Loa and the South Pole," *Journal of Geophysical Research*, vol. 100, no. 5, pp. 8967–8975, 1995.

[17] A. Virkkula, T. Mäkelä, R. Hillamo et al., "A simple procedure for correcting loading effects of aethalometer data," *Journal of the Air and Waste Management Association*, vol. 57, no. 10, pp. 1214–1222, 2007.

[18] N. Liu, Y. Yu, J. He, and S. Zhao, "Integrated modeling of urban-scale pollutant transport: application in a semi-arid urban valley, Northwestern China," *Atmospheric Pollution Research*, vol. 4, no. 3, pp. 306–314, 2013.

[19] L. Riuttanen, M. Hulkkonen, M. Dal Maso, H. Junninen, and M. Kulmala, "Trajectory analysis of atmospheric transport of fine particles, SO_2, NO_x and O_3 to the SMEAR II station in Finland in 1996–2008," *Atmospheric Chemistry and Physics*, vol. 13, no. 4, pp. 2153–2164, 2013.

[20] A. Sirois and J. W. Bottenheim, "Use of backward trajectories to interpret the 5-year record of PAN and O_3 ambient air concentrations at Kejimkujik National Park, Nova Scotia," *Journal of Geophysical Research*, vol. 100, no. 2, pp. 2867–2881, 1995.

[21] L. L. Ashbaugh, W. C. Malm, and W. Z. Sadeh, "A residence time probability analysis of sulfur concentrations at Grand Canyon National Park," *Atmospheric Environment Part A*, vol. 19, no. 8, pp. 1263–1270, 1985.

[22] M. D. Cheng, P. K. Hopke, L. Barrie, A. Rippe, M. Olson, and S. Landsberger, "Qualitative determination of source regions of aerosol in Canadian high Arctic," *Environmental Science & Technology*, vol. 27, no. 10, pp. 2063–2071, 1993.

[23] C. O. Justice, L. Giglio, S. Korontzi et al., "The MODIS fire products," *Remote Sensing of Environment*, vol. 83, no. 1-2, pp. 244–262, 2002.

[24] U. Jeong, J. Kim, H. Lee et al., "Estimation of the contributions of long range transported aerosol in East Asia to carbonaceous aerosol and PM concentrations in Seoul, Korea using highly time resolved measurements: a PSCF model approach," *Journal of Environmental Monitoring*, vol. 13, no. 7, pp. 1905–1918, 2011.

[25] V. P. Kabashnikov, A. P. Chaikovsky, T. L. Kucsera, and N. S. Metelskaya, "Estimated accuracy of three common trajectory statistical methods," *Atmospheric Environment*, vol. 45, no. 31, pp. 5425–5430, 2011.

[26] L. Zhu, X. Huang, H. Shi, X. Cai, and Y. Song, "Transport pathways and potential sources of PM10 in Beijing," *Atmospheric Environment*, vol. 45, no. 3, pp. 594–604, 2011.

[27] S. Byčenkiene, V. Ulevicius, and S. Kecorius, "Characteristics of black carbon aerosol mass concentration over the East Baltic region from two-year measurements," *Journal of Environmental Monitoring*, vol. 13, no. 4, pp. 1027–1038, 2011.

[28] K. Juda-Rezler, M. Reizer, and J. P. Oudinet, "Determination and analysis of PM10 source apportionment during episodes of air pollution in Central Eastern European urban areas: the case of wintertime 2006," *Atmospheric Environment*, vol. 45, no. 36, pp. 6557–6566, 2011.

[29] L. Morawska, Z. Ristovski, E. R. Jayaratne, D. U. Keogh, and X. Ling, "Ambient nano and ultrafine particles from motor vehicle emissions: characteristics, ambient processing and implications on human exposure," *Atmospheric Environment*, vol. 42, no. 35, pp. 8113–8138, 2008.

[30] A. Zwozdziak, L. Samek, I. Sowka, L. Furman, and M. Skrtowicz, "Aerosol pollution from small combustors in a village," *The Scientific World Journal*, vol. 2012, Article ID 956401, 8 pages, 2012.

[31] S. Byčenkienė, V. Ulevicius, N. Prokopčiuk, and D. Jasinevičienė, "Observations of the aerosol particle number concentration in the marine boundary layer over the south-eastern Baltic Sea region," *Oceanologia*, vol. 55, no. 3, pp. 573–598, 2013.